Dynamical model selection for quantum optomechanical systems

Jason F. Ralph,[1,*] Simon Maskell,[1,†] Kurt Jacobs,[2,3,4,‡] Muddassar Rashid,[5] Marko Toroš,[5] Ashley J. Setter,[5] and Hendrik Ulbricht[5]

[1] *Department of Electrical Engineering and Electronics, University of Liverpool, Brownlow Hill, Liverpool, L69 3GJ, UK.*
[2] *U.S. Army Research Laboratory, Computational and Information Sciences Directorate, Adelphi, Maryland 20783, USA.*
[3] *Department of Physics, University of Massachusetts at Boston, Boston, MA 02125, USA*
[4] *Hearne Institute for Theoretical Physics, Louisiana State University, Baton Rouge, LA 70803, USA*
[5] *Department of Physics and Astronomy, University of Southampton, University Road, Southampton, SO17 1BJ, UK*

(Dated: November 28, 2017)

This paper considers the problem of distinguishing between different dynamical models using continuous weak measurements; that is, whether the evolution is quantum mechanical or given by a classical stochastic differential equation. We examine the conditions that optimize quantum hypothesis testing, maximizing one's ability to discriminate between classical and quantum models. We set upper limits on the temperature and lower limits on the measurement efficiencies required to explore these differences, using experiments in levitated optomechanical systems as an example.

PACS numbers: 05.45.Mt, 03.65.Ta, 05.45.Pq
Keywords: levitated optomechanical systems, dynamical model selection, quantum state estimation, classical state estimation

Introduction.— There are a number of ways in which a system can be determined to be quantum mechanical. Typically, the system must be isolated from extraneous noise and operated at very low temperatures, so that the system is in a ground state or another low lying energy state. The system can be subjected to a series of individual or joint measurements to build up a picture of the state (as in interference experiments and state tomography [1–6]) or manipulated using an external field to demonstrate superposition states (such as avoided crossings in the observed energy spectra [7–10]). These experiments provide direct evidence of quantum behavior but they can be difficult to perform when the system has several degrees of freedom and large numbers of measurements are required. More efficient alternatives have been devised with the growth of quantum information as a subject area. Specific sequences of measurements can be applied to ascertain whether the system contains non-classical correlations (entanglement) associated with quantum behavior [11–13]. *Entanglement witnesses* do not necessarily allow an experimentalist to quantify the degree of entanglement, but they do allow her to say that entanglement is present and, hence, that the system is quantum mechanical rather than classical. All of these methods are intended to provide direct evidence that the system is manifestly non-classical: discrete energy levels, interference, superposition states, entanglement, etc..

An alternative approach is to try to determine whether the system *dynamics* are quantum rather classical. An elegant approach to this task is to use the technique of *quantum hypothesis testing* [14, 15]. In situations where direct experiments are not possible, or are beyond the reach of current experiments, this method can also be used to inform future work, explore regions of parameter space, and to focus experimental efforts. This is the motivation for the current paper.

In this letter, we use a quantum hypothesis testing approach, often referred to as *model selection* in classical Bayesian inference [16], with a continuous measurement interaction [17–19] to provide limits on two important experimental parameters: the effective temperature of the system and the efficiency of the continuous measurement. These parameters are relevant to a number of systems, including superconducting circuits [20–23]. However, we concentrate on experiments with levitated optomechanical systems [24–27]. Quantum behavior has not yet been established in these systems, and improving the understanding of where and when such evidence might be available is an important open question.

The ability to determine whether a system is quantum mechanical is important for many practical reasons, including applications in quantum information and metrology. However, there are important reasons why such questions have relevance to fundamental physics. Levitated optomechanical systems are a testbed for fundamental investigations. A nanoparticle is captured and held in a trapping potential, isolated from most of the effects of its environment. The trapped nanoparticle is extremely small, but orders of magnitude larger than an atom or a typical molecule. It can be cooled to very low temperatures and probed using the fields used to form the trap. A number of interesting experiments have been proposed or performed; including ultra-sensitive force measurements [33], fundamental tests of gravity [34], and testing the limits of quantum mechanics [28–30].

Experimental framework.— For our purposes, the important factors are: (i) a levitated nanoparticle is physi-

*Electronic address: jfralph@liverpool.ac.uk
†Electronic address: smaskell@liverpool.ac.uk
‡Electronic address: kurt.jacobs@umb.edu

cally large (with a radius several hundred to a few thousand times that of an atom); (ii) a nanoparticle has a high mass (six to eight orders of magnitude larger than an atom); (iii) the trap can be arranged to separate degrees of freedom in terms of frequency, thereby simplifying the system to one translational degree of freedom; and (iv) the particle is weakly coupled to a thermal environment and to a laser field that can be used to provide a continuous measurement of position. We will take parameters based on optomechanical spheres described in [35, 36], made from silica with radii $\simeq 25-100$nm and masses $m \simeq 10^{-18}-10^{-19}$kg. These are good candidates for study because they previously have been used in experiments to generate thermal squeezed states [35], measurements have been used to reconstruct (classical) Wigner functions [36], and they can realize the multiple-well potentials [37], which are found to maximize the discrimination between classical and quantum models.

Dynamical models.— In classical mechanics, the ability to observe a system continuously and control its motion is taken for granted. In quantum mechanics, measurement cannot be ignored. Conventionally, measurement projects onto an eigenstate of the measured operator. However, recent experimental advances have shown that probing a quantum system via its environment can provide a continuous measurement record and allow the construction of a *quantum trajectory* describing its motion [17–19]. This continuous measurement must be weak to allow Schrödinger evolution that is perturbed by the effect of the environment and the backaction of the measurement. Continuous measurement models have been studied theoretically for over twenty years and form the basis for incoherent quantum control [17–19], but it is only recently that the reconstruction of quantum trajectories have been demonstrated in experiments [20–23]. It is these quantum trajectories that are used here and compared to classical trajectories to extract probabilities for the two hypotheses (classical or quantum evolution).

A continuous quantum measurement process is usually modeled with a Stochastic Master Equation (SME) [17–19], which can be written as

$$\begin{aligned} d\rho_c &= -i\left[\hat{H},\rho_c\right]dt \\ &\quad + \sum_{r=1}^{m'}\left\{\hat{L}_r\rho_c\hat{L}_r^\dagger - \frac{1}{2}\left(\hat{L}_r^\dagger\hat{L}_r\rho_c + \rho_c\hat{L}_r^\dagger\hat{L}_r\right)\right\}dt \\ &\quad + \sum_{r=1}^{m'}\sqrt{\eta_r}\left(\hat{L}_r\rho_c + \rho_c\hat{L}_r^\dagger - \mathrm{Tr}(\hat{L}_r\rho_c + \rho_c\hat{L}_r^\dagger)\right)dW_r \end{aligned} \tag{1}$$

where ρ_c is the density matrix for the state of the system conditioned on the measurement record – the state (possibly mixed), which represents the current knowledge of the quantum state, $\hat{H}$ is the Hamiltonian of the system, dt is an infinitesimal time increment, and the operators $\hat{L}_r$ represent the effect of the environment and measurement. The measurement record for each of the operators $\hat{L}_r$ during a time step $t \to t+dt$ is given by, $y(t+dt)-y(t) = dy_r(t) = \sqrt{\eta_j}\mathrm{Tr}(\hat{L}_r\rho_c + \rho_c\hat{L}_r^\dagger)dt + dW_r$. η_r is the measurement efficiency; the ratio of the signal power due the measurement relative to the power of other extraneous sources of noise, where $\eta_r = 1$ is an ideal measurement and $\eta_r = 0$ is an unprobed environmental degree of freedom. Moreover, we will assume that dW_r are independent real Wiener processes, i.e. $dW_r dW_{r'} = \delta_{rr'}dt$. Physically, this SME represents a situation where the measurement environment decoheres sufficiently rapidly that no correlations build up between the state of the quantum system of interest and the environmental degrees of freedom (Markov approximation).

For the case considered here, the SME is given by (1) with three environmental operators ($m' = 3$): one measurement of the position (q) of the nanosphere within the trap, $\hat{L}_1 = \sqrt{8k}\hat{q}$, and two operators representing an unprobed thermal environment $\hat{L}_2 = \sqrt{(\bar{n}+1)\Gamma}\hat{a}^\dagger$ and $\hat{L}_3 = \sqrt{\bar{n}\Gamma}\hat{a}$ [38]; where $\hat{a}^\dagger$ and $\hat{a}$ are the usual harmonic oscillator raising and lowering operators, Γ is a decay rate ($\Gamma \ll \omega$), $\bar{n} = (\exp(\hbar\omega/k_BT)-1)^{-1}$ is the average thermal occupation number of a linear oscillator at temperature T, and k is the measurement strength for the continuous measurement interaction. The measurement efficiencies are $\eta_1 = \eta$, and $\eta_{2,3} = 0$ (unprobed). The measurement record for $\hat{L}_1$ is $dy(t) = \sqrt{8\eta k}\mathrm{Tr}(\rho_c(t)\hat{q})dt + dW$. For the purposes of this paper, we have selected a Hamiltonian that corresponds to a double well potential (a Duffing oscillator [39–41]),

$$\hat{H} = \frac{1}{2}\hat{p}^2 - \frac{1}{2}\omega^2\hat{q}^2 + \frac{1}{4}\mu\hat{q}^4 + g\cos(t)\hat{q} \tag{2}$$

where we have taken $\hbar = 1$, the mass is scaled so that $m = 1$, $\hat{p}$ is the momentum operator, ω is the angular frequency of a linear oscillator (although note that the sign of the linear term is reversed to create a barrier and a double well potential), μ is the nonlinear parameter, and g is the magnitude of an external periodic drive. This system has been widely studied in relation to chaotic dynamics in open quantum systems and the quantum-classical transition [39–45].

For the equivalent classical system, we take a Stochastic Differential Equation (SDE) for the position q and the momentum p of a classical particle,

$$\begin{aligned} dq &= pdt \\ dp &= -\mu q^3dt + \omega^2 qdt - \Gamma pdt + g\cos(t) \\ &\quad + \sqrt{2k}dY + \sqrt{2\Gamma k_BT}dU \end{aligned} \tag{3}$$

where the measurement record is $dy_c(t) = \sqrt{8\eta k}qdt + dW$ and we have again set $\hbar = 1$. Like dW, dY and dU are also real Weiner increments, $dY^2 = dU^2 = dt$, but they are uncorrelated so that $dWdU = dWdY = dYdU = 0$, and there is no backaction from the measurement on the state of the system in a classical measurement.

Model Selection.— Dynamical model selection requires that we take a measurement record from an initial point

$t = 0$ to the current time $t = t' = n\Delta t$, denoted by $\Delta y_{0:t'}$, where we now take finite intervals in time. We then calculate the probability that the underlying dynamical model is quantum (Q, the evolution is given by the SME (1)) or classical (C, the evolution is determined by the SDE (3)). The probabilities are calculated from an initial prior probability for each model $p_0(\mathrm{Q})$ and $p_0(\mathrm{C})$ assuming that the noise in each measurement increment is independent of the others,

$$p(\mathrm{Q}|\Delta y_{0:t'}) \propto p_0(\mathrm{Q}) \prod_{t=\Delta t:t'} p(\Delta y_t|\mathrm{Q}, \Delta y_{0:t-\Delta t}) \tag{4}$$

$$p(\mathrm{C}|\Delta y_{0:t'}) \propto p_0(\mathrm{C}) \prod_{t=\Delta t:t'} p(\Delta y_t|\mathrm{C}, \Delta y_{0:t-\Delta t}) \tag{5}$$

Since we only have two models as possible hypotheses, the probabilities should sum to one and the normalization condition is fixed by $p(\mathrm{Q}|\Delta y_{0:t'}) + p(\mathrm{C}|\Delta y_{0:t'}) = 1$. As such, the probabilities being calculated are the relative probabilities between the two dynamical models, which does not include the possibility of systematic errors. These limitations are considered in detail by Tsang in [15], where the different types of systematic errors are listed and discussed. This limitation does not invalidate the approach presented here. However, it does mean that experimental studies need to be careful to calibrate their systems fully and to verify that systematic errors are not present.

To calculate the probabilities, one can obtain data from a real system or, in the absence of an experiment, we can generate a specific realization of the measurement record $\Delta\tilde{y}_{0:t'}$ using one of the models, (1) or (3). This represents the measurement record that would be expected from an experiment. We then use $\Delta\tilde{y}_{0:t'}$ as an input to both of the dynamic models. In the case of the SME (1), the state is initialized in a mixed thermal state $\rho_c(0)$ at a temperature T. The record is used to construct an estimate of the Wiener increment

$$\Delta\tilde{W} = \Delta\tilde{y}_t - \sqrt{8\eta k}\mathrm{Tr}(\rho_c(t)\hat{q})\Delta t \tag{6}$$

which is then used in (1) to update the conditioned density matrix, representing the current estimate of the quantum state given $\Delta\tilde{y}_{0:t'}$. The probability update, $p(\Delta y_t|\mathrm{Q}, \Delta y_{0:t-\Delta t})$, is calculated using

$$p(\Delta\tilde{y}_t|\mathrm{Q}, \Delta\tilde{y}_{0:t-\Delta t}) = \frac{\exp\left(-(\Delta\tilde{W})^2/2\Delta t\right)}{\sqrt{2\pi\Delta t}} \tag{7}$$

The classical model requires the evolution of the probability density function (pdf) to be calculated, which is computationally expensive. We use an alternative approach here to solve the approximate problem using a sequential Monte Carlo method [46–48] known as a particle filter. The particle filter uses the fact that the evolution of the pdf can be approximated by the evolution of a finite number of candidate solutions or 'particles', each of which has a weight associated with it, where the weight evolves in such a way that a quantity averaged over all weighted particles approximates the expectation value for the quantity over the pdf. In this case, we take N particles, initialized with equal weight $w_0^{(i)} = 1/N$. Each particle has a position $q^{(i)}$ and a momentum $p^{(i)}$, initially selected from the same thermal distribution as that given by the thermal state for the quantum model. The particles then evolve according to the SDE (3) with independent noise sources. The weights are updated using

$$\tilde{w}_t^{(i)} = \frac{\exp\left(-\frac{(\Delta\tilde{y}_t - \sqrt{8\eta k}q^{(i)}\Delta t)^2}{2\Delta t}\right)}{\sqrt{2\pi\Delta t}} w_{t-\Delta t}^{(i)} \tag{8}$$

where the $\tilde{w}^{(i)}$'s are unnormalized weights after updating, and the probability for the classical model is approximated by $p(\Delta\tilde{y}_t|\mathrm{C}, \Delta\tilde{y}_{0:t'-\Delta t}) \propto \sum_{i=1}^{N} \tilde{w}_t^{(i)}$. As the system evolves, the values of some of the weights fall to near zero. The particles and the candidate solutions that they represent are then resampled using the current weight distribution as described in [16]. This evolution with periodic resampling allows the particle filter to be efficient whilst still retaining a diverse selection of candidate solutions. This makes the particle filter an ideal method for the estimation of a nonlinear dynamical process and it is the reason for considering it in a model selection context. In addition, the particle filter and other sequential Monte Carlo methods can be augmented to include the simultaneous estimation of system parameters [49] and they can be applied to quantum systems described by SMEs with uncertain parameters [50].

To ascertain the distinguishably of the two models, we calculate the confusion matrix for the two hypotheses [54], each point calculated over 100 individual runs. The confusion matrix is a standard method to evaluate a classification process, in that it provides a probability for getting the right result and for making an error. In our case, the confusion matrix is given by,

$$M_c = \begin{pmatrix} p(\mathrm{C}|\mathrm{C}) & p(\mathrm{C}|\mathrm{Q}) \\ p(\mathrm{Q}|\mathrm{C}) & p(\mathrm{Q}|\mathrm{Q}) \end{pmatrix} \tag{9}$$

where $p(\mathrm{C}|\mathrm{Q})$ is the probability of a Type II error (false negative, assuming that the classical hypothesis C is the default or null hypothesis) and $p(\mathrm{Q}|\mathrm{C})$ is the probability of a Type I error (false positive). More generally, one can generate a Receiver-Operator Characteristic (ROC) curve by varying the threshold probability above or below which each hypothesis is taken to be true [54], but here we take a uniform prior $p_0(\mathrm{Q}) = p_0(\mathrm{C}) = 1/2$ and fix the threshold to be one half.

Application to optomechanical systems.— For the case considered here, a one-dimensional potential with a trapped nanoparticle, we need to find the conditions where one can best discriminate between the two dynamical models. A number of different conditions were examined, for single well (linear and non-linear) and double well potentials. The optimum condition was found to

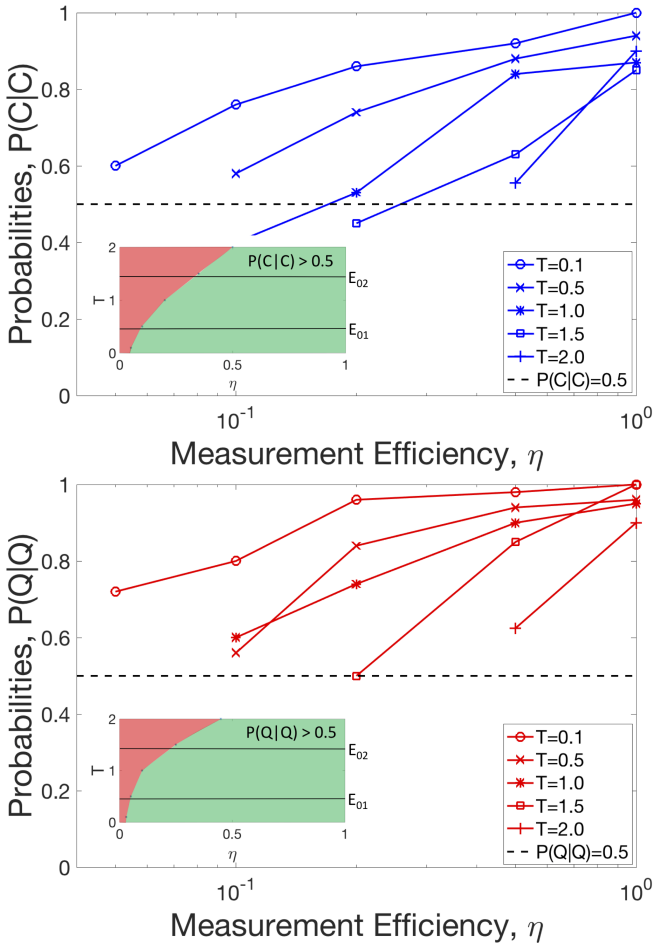

FIG. 1: (color online) Probabilities for correct identification of the dynamical evolution, $p(\mathrm{C}|\mathrm{C})$ and $p(\mathrm{Q}|\mathrm{Q})$, for different temperatures as a function of the measurement efficiency. Inserts show approximate regions where the models are distinguishable (green (light gray) shaded regions), as functions of temperature and measurement efficiency.

be a double-well potential where the wells were well separated in position and the barrier between the two wells was high enough for the classical particle to remain in one well for a reasonable period of time, before the environmental noise kicked it into the other well. In addition, the barrier also had to be low enough to prevent the quantum state for localizing in one or other of the wells. In practice, these conditions correspond to a symmetric double well potential where the quantum ground state lies below the barrier height but the first excited state is above the barrier. The classical system is always localized, in the sense that it is a point particle, but the pdf represented by the particles needs to be largely localized to one of the wells by the measurements. By contrast, a quantum state can only be localized to one of the wells if two of the low lying energy levels are below the barrier. If the barrier is sufficiently high, the lowest two energy states are formed from the symmetric and anti-symmetric superposition of localized well states, and a localized well state can be generated by combining these two energy levels [51]. If the first excited state lies above the barrier, then a superposition of this with the ground state will not be localized in one well. For the Duffing Hamiltonian (2), these conditions are met if $\omega = 1$, $\mu = 0.5$ and $g = 0$ (undriven oscillator), and we take $\Gamma = 0.05$, $k = 0.025$, $N = 500$. The quantum model uses Rouchon's integration method [52, 53] with non-commutative noise sources and a moving basis [39–41] with 60-100 linear oscillator states. The models are integrated over 100 cycles of the linear oscillator with 500-2000 time steps per oscillator cycle. The barrier height in this example is $\Delta E_b = 0.5\hbar\omega$, the two wells are separated in position by $\Delta q = 3\sqrt{\hbar/m\omega}$, the lowest two energy levels are separated by $\Delta E_{01} = 0.396\hbar\omega$, and the next excited states are separated by $\Delta E_{12} = 0.941\hbar\omega$ and $\Delta E_{23} = 1.061\hbar\omega$.

Figure 1 shows the probabilities contained in the confusion matrix for the correct detection of the dynamical models for different temperatures as a function of the measurement efficiency. In general, the probabilities for correctly identifying a quantum system, $P(Q|Q)$, are slightly higher than for the classical system, $P(C|C)$. At low temperatures $k_BT < \Delta E_{01}$ the distinguishability is excellent, approaching 100% even for measurement efficiencies $\eta \simeq 0.2$. This contrasts with a linear trap, where the probability of correctly distinguishing dynamical models was found to be limited to around 80%, even for very low temperatures and ideal measurements $\eta = 1.0$. Here, with two wells, both dynamical models show good distinguishability between quantum and classical behavior for temperatures $T \simeq 0.5$ ($k_BT \simeq \Delta E_{01}$) and measurement efficiencies $\eta > 0.2$, with some ability to distinguish between the two models for temperatures where the thermal energy is well above the first energy level separation and around the second transition, $k_BT \simeq 1.5\hbar\omega \sim 4\Delta E_{01}$, as long as $\eta > 0.5$. It should be noted that the ability to distinguish the models is dependent on the total time over which the measurement record is collected and the models integrated. Extending the integration time will improve the results, but the trap potential and the measurement interaction would need to be stable over the integration time, providing a trade-off between distinguishability and difficulties in collecting the measurement data.

Typical trapping frequencies in experiments are around 100kHz and masses of the nanoparticles are a few $\times\, 10^{-19}$kg [35, 36]. In this case, $\hbar\omega$ corresponds to a temperature of 0.77μK, and $T = 1.5 \simeq 1.16\mu$K, with the two wells separated by 0.2nm, smaller than the radius of the sphere. However, the accuracy of the measurement in such systems is typically very good, $\sim$ 1pm [35, 36]. It should be possible to measure the differences in position at the required precision to distinguish the two dynamical models, even at relatively high temperatures, $k_BT \sim 4\Delta E_{01}$, as long as $\eta > 0.5$. Experiments with levitated nanoparticles have reported temperatures around 450μK [55], well above the regime required, but experimental techniques are improving rapidly and tem-

peratures equivalent to $\bar{n} \sim 10 - 20$ are anticipated in the near future. Measurement efficiencies are more difficult to estimate from previous work since the values are not critical to the results presented and are not normally provided. However, for other systems, such as superconducting circuits [20–23] it is known that measurement efficiencies of at least $\eta \sim 0.4$ are achievable [21].

Conclusions.— This paper has examined how two dynamical models, one classical and one quantum mechanical, can be distinguished using continuous weak measurements. The approach can be used at temperatures above the minimum energy level separation of the quantum system and for systems with inefficient measurements. The paper has examined the use of dynamical model selection for experiments on levitated optomechanical systems. In this application, the problem of determining whether an object is evolving quantum mechanically is challenging. However, limits have been provided for two key experimental parameters (temperature and measurement efficiency) for quantum behaviour to be detected reliably. The upper limit for the temperature dictates that the thermal energy can be several times the lowest energy level separation, as long as the measurement efficiency is greater than 50%.

Acknowledgments.— JFR would like to thank H. M. Wiseman, P. Barker, and M. Flinders for useful and informative discussions. MR, MT, AS and HU acknowledge funding by the Leverhulme Trust (RPG-2016-046) and the Foundational Questions Institute (FQXi) and AS acknowledges support by the Engineering and Physical Sciences Research Council (EPSRC) under Centre for Doctoral Training grant EP/L015382/1.

[1] O. Nairz, M. Arndt, A. Zeilinger. *American Journal of Physics* **71**, 319-325 (2003).
[2] S. Gerlich, S. Eibenberger, M. Tomandl, S. Nimmrichter, K. Hornberger, P.J. Fagan, J. Tuxen, M. Mayor, M. Arndt, *Nature Communications* **2**, 263 (2011).
[3] D.T. Smithey, M. Beck, M. G. Raymer, A. Faridani, *Physical Review Letters* **70**, 1244-1247 (1993).
[4] A. I. Lvovsky, H. Hansen, T. Aichele, O. Benson, J. Mlynek, S. Schiller, *Physical Review Letters* **87**, 050402 (2001).
[5] C.F. Roos, G. P. T. Lancaster, M. Riebe, H. Haffner, W. Hansel, S. Gulde, C. Becher, J. Eschner, F. Schmidt-Kaler, R. Blatt, *Physical Review Letters* **92**, 220402 (2004).
[6] K. J. Resch, P. Walther, A. Zeilinger, *Physical Review Letters* **94**, 070402 (2005).
[7] Y. Nakamura, C. D. Chen, J. S. Tsai, *Physical Review Letters* **79**, 2328 (1997).
[8] J.R. Friedman, V. Patel, W. Chen, S.K. Tolpygo, J.E. Lukens, *Nature* **406**, 43 (2000).
[9] C.H. van der Wal, A.C.J. ter Haar, F.K. Wilhem, R.N. Schouten, C.J.P.M. Harmans, T.P. Orlando, S. Lloyd, J.E. Mooij, *Science* **290**, 773 (2000).
[10] J.M. Martinis, S. Nam, J. Aumentado, C. Urbina, *Physical Review Letters* **89**, 117901 (2002)
[11] M. Barbieri, F. De Martini, G. Di Nepi, Paolo Mataloni, G. M. D'Ariano, C. Macchiavello, *Physical Review Letters* **91**, 227901 (2003).
[12] M. Bourennane, M. Eibl, C. Kurtsiefer, S. Gaertner, H. Weinfurter, O. Ghne, P Hyllus, D. Bru, M. Lewenstein, A. Sanpera, *Physical Review Letters* **92**, 087902 (2004).
[13] C.-Y.Lu, X.-Q. Zhou, O Ghne, W.-B. Gao, J. Zhang, Z.-S. Yuan, A Goebel, T. Yang, J.-W. Pan, *Nature Physics* **3**, 91-95 (2007).
[14] M. Tsang, *Phys. Rev. Lett.* 108, 170502 (2012).
[15] M. Tsang, *Quantum Measurements and Quantum Metrology* 1, 84 (2013).
[16] N. Gordon, S. Maskell, T. Kirubarajan, *Proc. of SPIE Signal and Data Processing of Small Targets*, **4728**, p.439-449 (2002).
[17] V. P. Belavkin *Reports on Mathematical Physics* **43**, 353 (1999), and references contained therein.
[18] H. M. Wiseman, G. J. Milburn, 'Quantum Measurement and Control' (Cambridge University Press, Cambridge, 2010).
[19] K. Jacobs 'Quantum Measurement Theory and Its Applications' (Cambridge University Press, Cambridge, 2014).
[20] K. W. Murch, S. J. Weber, C. Macklin, I. Siddiqi, *Nature* **502**, 211 (2013).
[21] S. J. Weber, A. Chantasri, J. Dressel, A. N. Jordan, K. W. Murch, I. Siddiqi, *Nature* **511**, 570 (2014).
[22] P. Six, P. Campagne-Ibarcq, L. Bretheau, B. Huard, P. Rouchon, *54th IEEE Conference on Decision and Control Conference (CDC)* (2015).
[23] P. Campagne-Ibarcq, P. Six, L. Bretheau, A. Sarlette, M. Mirrahimi, P. Rouchon, B. Huard, *Physical Review X* **6**, 011002 (2016).
[24] A. Ashkin, *Physical Review Letters* **24**, 156 (1970).
[25] S. Mancini, D. Vitali, P. Tombesi, *Physical Review Letters* **80**, 688 (1998).
[26] M. Gangl, H. Ritsch, *Physical Review A* **61**, 011402 (1999).
[27] V. Vuletic, S. Chu, *Physical Review Letters* **84**, 3787 (2000).
[28] A. Bassi, G. C. Ghirardi, *Physics Reports* **379**, 257-426 (2003).
[29] A. Bassi, K. Lochan, S. Satin, T. P. Singh, H. Ulbricht, *Reviews of Modern Physics* **85**, 471527 (2013).
[30] S. Bera, B. Motwani, T. P. Singh, H. Ulbricht, *Scientific Reports* **5**, 7664 (2015).
[31] O.Romero-Isart, A. C. Pflanzer, M. L. Juan, R. Quidant, N. Keisel, M. Aspelmeyer, J. I. Cirac, *Physical Review A* **83**, 013803 (2011).
[32] B. A. Stickler, S. Nimmrichter, L. Martinetz, S. Kuhn, M. Arndt, K. Hornberger, arXiv:1605.05674v1 (2016).
[33] A. A. Geraci, S. B. Papp, J. Kitching, *Physical Review Letters* **105**, 101101 (2010).
[34] A. Arvanitaki, A. A. Geraci, *Physical Review Letters* **110**, 071105 (2013).
[35] M. Rashid, T Tufarelli, J. Bateman, J. Vovrosh, D. Hempston, M. S. Kim, H. Ulbricht, *Physical Review Letters* **117**, 273601 (2016).
[36] M. Rashid, M. Toros, H. Ulbricht, arXiv:1707.07859 (2017).

[37] L. Rondin, J. Gieseler, F. Ricci, R. Quidant, C. Dellago. L. Novotny, *Nature Nanotechnology*, 10.1038/NNANO.2017.198 (2017)/

[38] T.P. Spiller, B.M. Garraway, I.C. Percival, *Physics Letters A*, **179**, 63 (1993).

[39] R. Schack, T. A. Brun, I. C. Percival. *Journal of Physics A: Mathematical and General* **28**, 5401 (1995).

[40] T. A. Brun, I. C. Percival, R. Schack, *Journal of Physics. A: Mathematical and General* **29** 2077 (1996).

[41] J. F. Ralph, K. Jacobs, M. J. Everitt, *Physical Review A* **95**, 012135 (2017).

[42] T. Bhattacharya, S. Habib, K. Jacobs, *Physical Review A* **7** 042103 (2003).

[43] M. J. Everitt, T. D. Clark, P. B. Stiffell, J. F. Ralph, A. R. Bulsara, C. J. Harland. *New Journal of Physics* **7** 64 (2005).

[44] J. K. Eastman, J. J. Hope, A. R. R. Carvalho. *Emergence of chaos controlled by quantum noise*, arXiv:1604.03494 (2016).

[45] B. Pokharel, P. Duggins, M. Misplon, W. Lynn, K. Hallman, D. Anderson, A. Kapulkin, A. K. Pattanayak, *Dynamical complexity in the quantum to classical transition*, arXiv:1604.02743 (2016).

[46] N. Gordon, D. Salmond, A. F. Smith, *IEE Proceedings F Radar Signal Processing*, **140**, 107113 (1993).

[47] A. Doucet, N. De Freitas, and N. Gordon, Eds., 'Sequential Monte Carlo Methods in Practice' (Springer, New York, 2001).

[48] M. Arulampalam, S. Maskell, N. Gordon, T. Clapp, *IEEE Transactions on Signal Processing* **50**, 241-254, (2002).

[49] P. L. Green, S Maskell, *Mechanical Systems and Signal Processing*, **93**, 379396 (2017).

[50] J.F. Ralph, S. Maskell, K. Jacobs, *Physical Review A* **96**, 052306 (2017).

[51] M. J. Everitt, T. D. Clark, P. B. Stiffell, A. Vourdas, J. F. Ralph, R. J. Prance,H. Prance *Physical Review A* **69**, 043804 (2004).

[52] H. Amini, M. Mirrahimi, P. Rouchon, *in Proc. 50th IEEE Conf. on Decision and Control*, pp. 6242-6247 (2011).

[53] P. Rouchon, J. F. Ralph, *Physical Review A* **91**, 012118 (2015).

[54] D. J. Hand, R. J. Till, *Machine Learning* **45**, 171-186 (2001).

[55] V. Jain, J. Gieseler, C. Moritz, C. Dellago, R. Quidant, L. Novotny, *Physical Review Letters* **116**, 243601 (2016).